RESEARCH

Mice lacking adenosine 2A receptor reveal increased severity of MCD-induced NASH

Jing Zhou[1], Honggui Li[1], Yuli Cai[1,2], Linqiang Ma[1,3,4], Destiny Matthews[1], Bangchao Lu[1,5], Bilian Zhu[1,6], Yanming Chen[6], Xiaoxian Qian[7], Xiaoqiu Xiao[4], Qifu Li[3], Shaodong Guo[1], Yuqing Huo[8], Liang Zhao[1,9], Yanan Tian[10], Qingsheng Li[11] and **Chaodong Wu[1]**

[1]Department of Nutrition and Food Science, Texas A&M University, College Station, Texas, USA
[2]Department of Endocrinology, Renmin Hospital, Wuhan University, Wuhan, Hubei, China
[3]Department of Endocrinology, The First Affiliated Hospital of Chongqing Medical University, Chongqing, China
[4]The Laboratory of Lipid & Glucose Metabolism, The First Affiliated Hospital of Chongqing Medical University, Chongqing, China
[5]Department of Geriatrics, Nanjing Drum Tower Hospital, the Affiliated Nanjing Hospital of Nanjing University Medical School, Nanjing, Jiangshu, China
[6]Department of Endocrinology, The Third Affiliated Hospital of Sun Yat-sen University, Guangzhou, Guangdong, China
[7]Department of Cardiology, The Third Affiliated Hospital of Sun Yat-sen University, Guangzhou, Guangdong, China
[8]Vascular Biology Center, Department of Cellular Biology and Anatomy, Medical College of Georgia, Augusta University, Augusta, Georgia, USA
[9]Beijing Advanced Innovation Center for Food Nutrition and Human Health, College of Food Science & Nutritional Engineering, China Agricultural University, Beijing, China
[10]Department of Veterinary Physiology and Pharmacology, College of Veterinary Medicine, Texas A&M University, College Station, Texas, USA
[11]Nebraska Center for Virology, School of Biological Sciences, University of Nebraska-Lincoln, Lincoln, Nebraska, USA

Correspondence should be addressed to C Wu: cdwu@tamu.edu

*(J Zhou and H Li contributed equally to this work)

Abstract

Adenosine 2A receptor (A_{2A}R) exerts a protective role in obesity-related non-alcoholic fatty liver disease. Here, we examined whether A_{2A}R protects against non-alcoholic steatohepatitis (NASH). In C57BL/6J mice, feeding a methionine- and choline-deficient diet (MCD) resulted in significant weight loss, overt hepatic steatosis, and massive aggregation of macrophages in the liver compared with mice fed a chow diet. MCD feeding also significantly increased the numbers of A_{2A}R-positive macrophages/Kupffer cells in liver sections although decreasing A_{2A}R amount in liver lysates compared with chow diet feeding. Next, MCD-induced NASH phenotype was examined in A_{2A}R-disrupted mice and control mice. Upon MCD feeding, A_{2A}R-disruptd mice and control mice displayed comparable decreases in body weight and fat mass. However, MCD-fed A_{2A}R-disrupted mice revealed greater liver weight and increased severity of hepatic steatosis compared with MCD-fed control mice. Moreover, A_{2A}R-disupted mice displayed increased severity of MCD-induced liver inflammation, indicated by massive aggregation of macrophages and increased phosphorylation states of Jun-N terminal kinase (JNK) p46 and nuclear factor kappa B (NFκB) p65 and mRNA levels of tumor necrosis factor alpha, interleukin-1 beta, and interleukin-6. *In vitro*, incubation with MCD-mimicking media increased lipopolysaccharide (LPS)-induced phosphorylation states of JNK p46 and/or NFκB p65 and cytokine mRNAs in control macrophages and RAW264.7 cells, but not primary hepatocytes. Additionally, MCD-mimicking media significantly increased lipopolysaccharide-induced phosphorylation states of p38 and NFκB p65 in A_{2A}R-deficient macrophages, but insignificantly decreased lipopolysaccharide-induced phosphorylation states of JNK p46 and NFκB p65 in A_{2A}R-deficient hepatocytes. Collectively, these results suggest that A_{2A}R disruption exacerbates MCD-induced NASH, which is attributable to, in large part, increased inflammatory responses in macrophages.

Key Words

- adenosine 2A receptor
- non-alcoholic steatohepatitis
- lipodystrophy
- macrophage

Journal of Endocrinology (2019) **243**, 199–209

https://joe.bioscientifica.com
https://doi.org/10.1530/JOE-19-0198

Introduction

Non-alcoholic fatty liver disease (NAFLD) is characterized by excessive fat deposition in hepatocytes (steatosis) (Browning *et al.* 2004, Sanyal 2005). When the liver displays overt inflammatory damage due to fat deposition and inflammatory mediators from extrahepatic tissues, simple steatosis progresses to non-alcoholic steatohepatitis (NASH) as the advanced form of NAFLD (Cohen *et al.* 2011, Chalasani *et al.* 2018). Epidemiological data indicate that NASH affects 1.5–6.45% of the general populations (Younossi *et al.* 2016, Estes *et al.* 2018). Alarmingly, the incidence of NASH in both adults and children is rising continuously due to ongoing epidemics of obesity (Younossi *et al.* 2016, Estes *et al.* 2018). NASH is one of the most common causes of liver cirrhosis and hepatocellular carcinoma (Bugianesi *et al.* 2002, Marrero *et al.* 2002, Powell *et al.* 2005, Starley *et al.* 2010). To date, there is no effective treatment for NASH (Neuschwander-Tetri 2010, Chalasani *et al.* 2018).

Because NAFLD is highly prevalent in obese populations (Younossi *et al.* 2016, Estes *et al.* 2018), obesity-associated inflammation is accepted as a critical factor that initiates or exacerbates NAFLD. As supported by evidence from both human and animal studies, inflammation can impair hepatic insulin resistance and dysregulate hepatic fat metabolism, which in turn brings about pathological increases in hepatocyte fat deposition (Kang *et al.* 2008, Odegaard *et al.* 2008, Menghini *et al.* 2009). In addition, obesity-associated adipose tissue dysfunction has also been implicated to play a critical role in development of NAFLD. Indeed, this role of dysfunctional adipose tissue is highlighted by the 'second-hit' hypothesis. In support of this, adipocyte-specific overexpression of monocyte chemoattractant protein-1 (MCP1), an inflammatory molecule upregulated in adipose tissue of obese mice and human subjects, mediates the effect of adipose tissue inflammation to bring about an increase in hepatic triglyceride content (Kamei *et al.* 2006). These results and many others suggest that dysfunctional adipose tissue contributes to hepatic steatosis by increasing the delivery of fatty acid flux to the liver (Tilg & Moschen 2010) and by impairing liver insulin signaling through adipose tissue-driven inflammation (Kelley *et al.* 2003, Schaffler *et al.* 2005). During obesity, however, inflammation exists in both the liver and adipose tissue (Xu *et al.* 2014, Guo *et al.* 2016) and complicates with fat deposition, for example, adiposity and hepatic steatosis. This makes it difficult to separate the effects of inflammation from those of fat deposition. Furthermore, increased adiposity, when displaying fat composition characterized by an elevation of palmitoleate, can promote hepatic steatosis, but decrease liver inflammation (Huo *et al.* 2012). Given this, there is a critical need to better understand the role of inflammation in regulating NAFLD/NASH in the absence of obesity.

Adenosine 2A receptor ($A_{2A}R$) is one of the four adenosine receptors that belong to the superfamily of G-protein-coupled receptors and displays powerful anti-inflammatory effects in immune cells such as macrophages and neutrophils (Gessi *et al.* 2000, Haskó *et al.* 2008). Previous studies have validated a critical role for $A_{2A}R$ in the pathophysiology of NAFLD/NASH. Specifically, $A_{2A}R$ activation is shown to ameliorate NASH phenotype in both rats and mice (Imarisio *et al.* 2012, Alchera *et al.* 2017). In contrast, using $A_{2A}R$-disrupted mice, Cai *et al.* provide complementary evidence to support a protective role for $A_{2A}R$ in NAFLD (Cai *et al.* 2018), although the study by Csoka *et al.* suggests a contradictory role for $A_{2A}R$ in obesity and NAFLD (Csóka *et al.* 2017). Of importance, the protective role for $A_{2A}R$ is largely attributed to the effect of $A_{2A}R$ on suppressing inflammation derived from lipotoxicity (Imarisio *et al.* 2012, Alchera *et al.* 2017). However, it is not clear in the liver how the $A_{2A}R$ is altered by inflammation in the absence of obesity as it relates to development and progression of NAFLD/NASH. In the present study, we examined the expression of $A_{2A}R$ in livers of mice fed a methionine- and choline-deficient diet (MCD). We also examined the effect of $A_{2A}R$ disruption on MCD-induced NASH phenotype and examined the effects of MCD-mimicking media on the proinflammatory responses in both hepatocytes and macrophages.

Materials and methods

Animal experiments

$A_{2A}R$-disrupted ($A_{2A}R^{-/-}$ or $A_{2A}R^{+/-}$) mice, in which $A_{2A}R$ was disrupted in all cells, and their wild-type (WT) littermates ($A_{2A}R^{+/+}$ mice) were generated as previously described (Cai *et al.* 2018). Additional C57BL/6J mice were obtained from the Jackson Laboratory. All mice were maintained on a 12:12-h light–darkness cycle (lights on at 06:00). Study 1: male C57BL/6J mice, at 9–10 weeks of age (when body weight was greater than 20 g), were fed an MCD for 5 weeks or maintained on a chow diet (CD) to examine $A_{2A}R$ abundance in relation to diet-induced NASH. Study 2: both male and female $A_{2A}R$-disrupted mice and $A_{2A}R^{+/+}$ mice, at 9–10 weeks of age, were fed an MCD for 5 weeks to induce NASH (Rinella *et al.* 2008, Luo *et al.* 2018).

https://joe.bioscientifica.com
https://doi.org/10.1530/JOE-19-0198

All diets are products of Research Diets, Inc. At 1 day prior to harvest, all mice were subjected to EchoMRI™ analyzer (EchoMRI LLC, Houston, TX, USA) to measure body composition. After the feeding period, all mice were fasted for 4 h before killing for collection of blood and tissue samples as previously described (Guo *et al.* 2010, Huo *et al.* 2010, Cai *et al.* 2018). The levels of plasma alanine aminotransferase (ATL) were measured using an assay kit (BioVision, Inc. Milpitas, CA, USA). These protocols were approved by the Institutional Animal Care and Use Committee of Texas A&M University.

Histological and immunohistochemical analyses

The sections of paraffin-embedded liver blocks were stained with H&E and/or stained for F4/80 expression with rabbit anti-F4/80 antibodies (1:100) (AbD Serotec, Raleigh, NC, USA). Also, co-staining of F4/80 (rat anti-mouse, MCA497, Bio-Rad) and $A_{2A}R$ (7F6-G5-A2, Cat# sc-32261, Santa Cruz Biotechnology, Inc.) in liver sections was evaluated by double immunofluorescent labeling according to the manufacturer's instructions (Vector Laboratories, Inc. Burlingame, CA, USA) as previously described (Pei *et al.* 2018). Following staining, images were obtained using Leica TCS SPE Confocal Microscope System. The sections of frozen livers were stained with Oil Red O as previously described (Guo *et al.* 2016).

Cell culture and treatment

Primary mouse hepatocytes were isolated from male $A_{2A}R^{-/-}$ mice and $A_{2A}R^{+/+}$ mice, at 11–12 weeks of age, using a collagenase digestion method as previously described (Cai *et al.* 2018, Luo *et al.* 2018). After attachment, hepatocytes were further incubated in M199 supplemented with 10% fetal bovine serum (FBS) and 100 U/mL penicillin and 100 µg/mL streptomycin for 24 h. Thereafter, hepatocytes were incubated in MCD-mimicking media (US Biological Life Sciences, Salem, MA, USA) for an additional 24 h. Prior to harvest, hepatocytes were treated with or without lipopolysaccharide (LPS, 100 ng/mL) for 30 min. Cell lysates were prepared for Western blot analysis. Also, bone marrow cells were isolated from male $A_{2A}R^{-/-}$ mice and $A_{2A}R^{+/+}$ mice, at 11–12 weeks of age, and differentiated into macrophages (BMDM) as previously described (Xu *et al.* 2014). After differentiation, BMDM were incubated with MCD-mimicking media for 24 h and treated with or without LPS (100 ng/mL) for the last 30 min. Cell lysates were measured for proinflammatory signaling using Western blot analysis. For a confirmatory study, RAW264.7 cells were treated with MCD-mimicking media and/or control media, and assayed for proinflammatory signaling and cytokine expression same as BMDM.

Western blot analysis

Frozen liver tissues and cultured cells were prepared in a lysis buffer containing 50 mM HEPES (pH 7.4), 10 mM EDTA, 50 mM sodium pyrophosphate, 0.1 M sodium fluoride, 10 mM sodium orthovanadate, 2 mM phenylmethylsulfonyl fluoride, 10 µg/mL aprotinin, 10 µg/mL leupeptin, 2 mM benzamidine, and 1% Triton X-100. After protein electrophoresis and transfer, immunoblots were performed using rabbit anti-serum as primary antibody at a 1:1000 dilution. This dilution was used for each of the primary antibodies used for the present study. After washing, the blot was incubated with a 1:10,000 dilution of goat anti-rabbit horseradish peroxidase-conjugated secondary antibody and followed by a chemiluminescent kit (Immobilon™ Western; EMD Millipore) as described (Qi *et al.* 2017). GAPDH was used as a loading control. The maximum intensity of each band was quantified using ImageJ software. Protein amount of αSMA and/or $A_{2A}R$ was normalized to GAPDH and adjusted relative to the average of CD-fed mice. Similarly, ratios of Pp46/p46 and/or Pp65/65 were normalized to GAPDH and adjusted relative to the average of CD-fed WT mice, MCD-fed $A_{2A}R^{+/+}$ mice, or control medium-treated primary hepatocytes or BMDM from $A_{2A}R^{+/+}$ mice, which was arbitrarily set as 1 (AU). Antibodies against Pp46, p46, Pp65, p65, αSMA, and $A_{2A}R$ were products of Cell Signaling.

RNA isolation, reverse transcription, and real-time PCR

Total RNA was isolated from liver tissues. Reverse transcription was performed using the GoScript™ Reverse Transcription System (Promega) and real-time PCR analysis was performed using SYBR Green (LightCycler® 480 system; Roche) (Guo *et al.* 2012, 2013). The mRNA levels were analyzed for tumor necrosis factor alpha (*Tnfa*), interleukin 1 beta (*Ilb*), *Il6*, fatty acid synthase (*Fas*), carnitine palmitoyltransferase 1a (*Cpt1a*), and sterol regulatory element-binding protein 1c (*Srebp1c*). A total of 0.1 µg RNA was used for the determination. Results were normalized to 18s ribosomal RNA and plotted as relative expression to the average of MCD-fed $A_{2A}R^{+/+}$ mice, which was set as 1. Primer sequences are available upon request.

https://joe.bioscientifica.com
https://doi.org/10.1530/JOE-19-0198

Statistical methods

Numeric data are presented as means ± S.E.M. (standard error). Statistical significance was assessed by unpaired, two-way ANOVA (for comparisons including three or more groups) and/or two-tailed Student's *t* tests (for variables only involving two groups). Differences were considered significant at the two-tailed $P<0.05$. Tukey's range test was used as a *post hoc* test.

Results

MCD feeding induces lipoatrophy and severe NASH in mice

Feeding a high-fat diet (HFD) to C57BL/6J mice induces hepatic steatosis and inflammation that are associated with obesity and increased adiposity (Cai *et al.* 2018, Luo *et al.* 2018). In this type of mouse model, dysfunctional adipose tissue is thought to also contribute to NAFLD phenotype. Considering the existence of steatohepatitis in human subjects without obesity, we sought to feed male C57BL/6J mice an MCD and examined hepatic steatosis and inflammation in the presence of lipoatrophy. Compared with CD-fed male mice, MCD-fed male C57BL/6J mice revealed significant decreases in food intake and body weight (Fig. 1A and B). Additionally, MCD-fed mice displayed nearly no fat mass (Fig. 1C). When NASH phenotype was analyzed, the levels of plasma alanine aminotransferase (ALT) in MCD-fed mice were significantly increased compared with those in CD-fed mice (Fig. 1D). In contrast, MCD-fed mice revealed significantly decreased liver weight relative to CD-fed mice (Fig. 1E). Consistent with NASH phenotype, liver sections of MCD-fed mice displayed overt hepatic steatosis and revealed mass aggregation of F4/80+ macrophages (Fig. 1F). In addition, liver lysates of MCD-fed mice showed significant increases in the phosphorylation states of JNK1 p46 and the amount of αSMA, a marker of liver fibrosis (Fig. 1G). These results validate MCD-fed mice as a model of NASH, which reveals hepatic steatosis and severe inflammation in the presence of lipoatrophy.

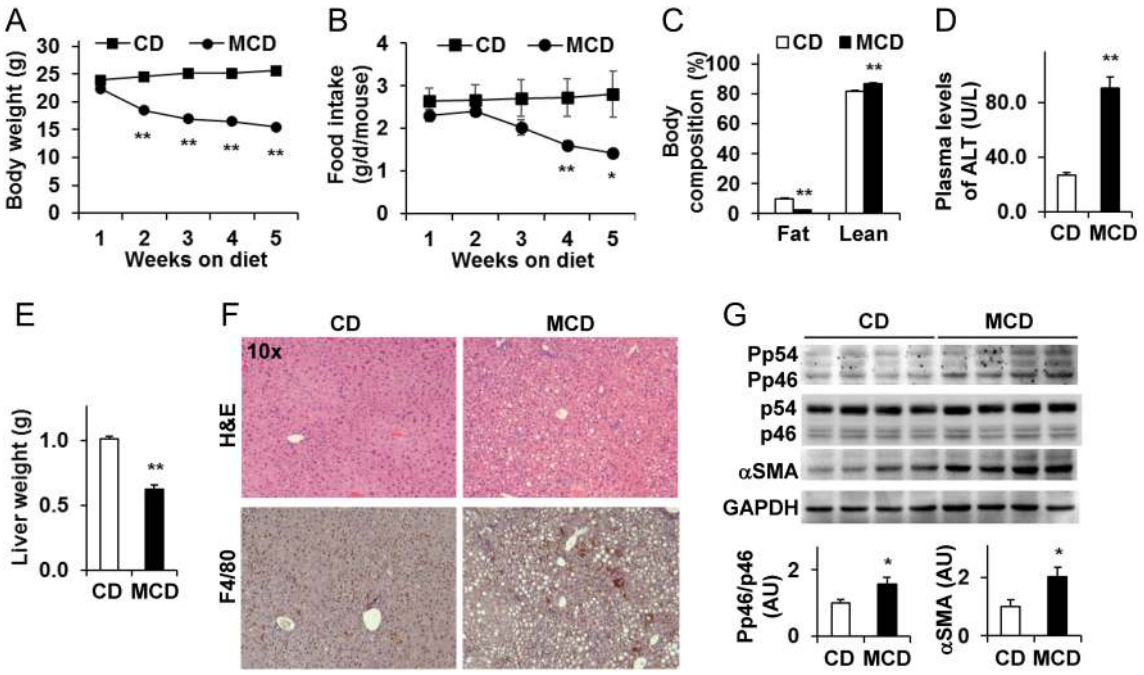

Figure 1
MCD feeding induces severe hepatic steatosis and inflammation while causing lipoatrophy. Male C57BL/6J mice, at 9–10 weeks of age, were fed a methionine- and choline-deficient (MCD) for 5 weeks or maintained on a chow diet (CD). (A and B) Body weight was measured during the feeding period (A). Also, foods consumed by the mice were recorded during the feeding period and used to calculate food intake (B). (C) At 1 day prior to the end of feeding period, body composition of the mice was analyzed using an EchoMRI analyzer. (D) Plasma levels of alanine aminotransferase (ALT). (E) Liver weight was measured after harvest of mice. (F) Liver sections were stained with H&E or for F4/80 expression. (G) Liver lysates were examined for the phosphorylation states of JNK p46 and the amount of αSMA. Bar graphs, quantification of blots. For A, B, C, D, E and G, numeric data are means ± S.E.M. (standard error), $n = 8–10$. AU, arbitrary unit. $^{*}P < 0.05$ and $^{**}P < 0.01$ MCD vs CD (in D, E, and G) for the same time point (in A and B) or for the same type of mass (in C). A full colour version of this figure is available at https://doi.org/10.1530/JOE-19-0198.

MCD feeding induces NASH and alters hepatic $A_{2A}R$ expression in mice

We showed before that hepatic $A_{2A}R$ expression was increased in mice with obesity-associated NAFLD and validated the increase in $A_{2A}R$ expression as a defensive response (Cai *et al.* 2018). Here we examined hepatic $A_{2A}R$ expression in MCD-fed mice. Unlike the changes in HFD-fed mice, the amount of $A_{2A}R$ in liver lysates of MCD-fed C57BL/6 mice was decreased compared with that in CD-fed mice (Fig. 2A). Next, we used immunofluorescent staining to examine the expression pattern of $A_{2A}R$ in liver macrophages/Kupffer cells; given that liver sections of MCD-fed C57BL/6J mice displayed marked aggregation of F4/80$^+$ cells. Compared with those of CD-fed mice, liver sections of MCD-fed mice contained much more $A_{2A}R$-postive cells (Fig. 2B), most of which were F4/80$^+$ cells (macrophages/Kupffer cells). Together, these results suggest that during MCD-induced NASH the liver revealed increased $A_{2A}R$ expression in macrophages although $A_{2A}R$ expression was decreased in liver lysates.

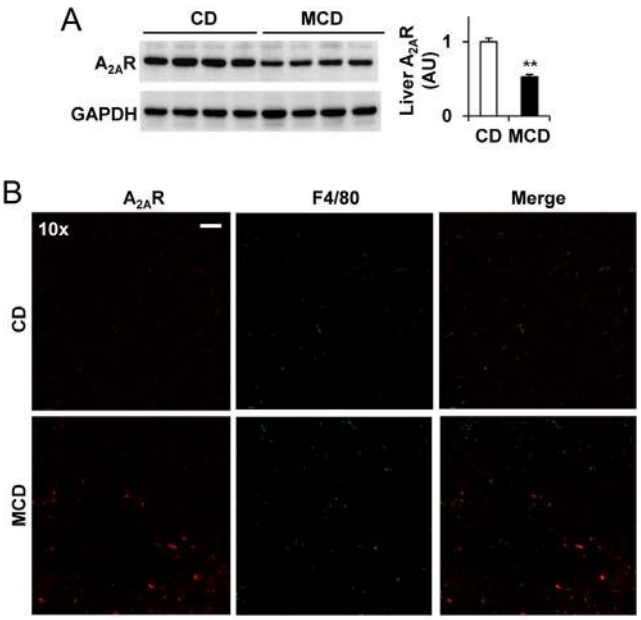

Figure 2
MCD feeding increases $A_{2A}R$ expression in liver macrophages/Kupffer cells although decreasing liver $A_{2A}R$ abundance. Male C57BL/6J mice, at 9–10 weeks of age, were fed an MCD for 5 weeks or maintained on a CD. (A) Liver lysates were examined for $A_{2A}R$ amount using Western blot analysis. Bar graph, quantification of blots. Data are means ± S.E.M. n = 6–10. AU, arbitrary unit. $^{**}P < 0.01$ MCD vs CD. (B) Liver sections were examined for the expression of F4/80 and/or $A_{2A}R$ using immunofluorescent staining. The scale bar is 75 µm for 10× images. A full colour version of this figure is available at https://doi.org/10.1530/JOE-19-0198.

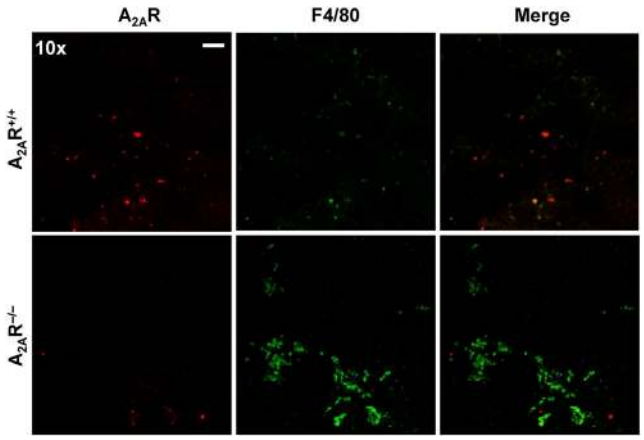

Figure 3
Validation of liver $A_{2A}R$ disruption. Male $A_{2A}R^{-/-}$ mice and $A_{2A}R^{+/+}$ mice, at 9–10 weeks of age, were fed an MCD for 5 weeks or maintained on a CD. After sacrifice of mice, liver sections were prepared and subjected to immunofluorescent staining of $A_{2A}R$ and/or F4/80 expression. The scale bar is 75 µm for 10× images. A full colour version of this figure is available at https://doi.org/10.1530/JOE-19-0198.

Validation of $A_{2A}R$ disruption in livers of MCD-fed mice

MCD feeding altered liver $A_{2A}R$ expression. Next, we sought to use $A_{2A}R$-disrupted mice to examine whether $A_{2A}R$ exerts a protective role in the pathogenesis of MCD-induced NASH. Initially, we analyzed $A_{2A}R$ expression in liver sections of MCD-fed male $A_{2A}R^{-/-}$ mice and their wild-type (WT, $A_{2A}R^{+/+}$) littermates. Upon immunofluorescent staining, liver sections of MCD-fed male $A_{2A}R^{+/+}$ mice displayed significant amount of $A_{2A}R$-postive cells, many of which were F4/80$^+$ macrophages/Kupffer cells. In contrast, liver sections of MCD-fed male $A_{2A}R^{-/-}$ mice contained almost no $A_{2A}R$-postive cells, but revealed significant increases in the numbers of F4/80-positive cells compared with those of MCD-fed male $A_{2A}R^{+/+}$ mice (Fig. 3). These results validated $A_{2A}R$ deficiency and confirmed that MCD feeding induced mass macrophage aggregation.

$A_{2A}R$ disruption does not alter the effect of MCD feeding on decreasing body weight and abdominal fat mass

$A_{2A}R$ disruption exacerbates HFD-induced weight gain (Cai *et al.* 2018). However, it is not clear whether $A_{2A}R$ disruption influences MCD-induced weight loss. We measured body weight and analyzed body composition of MCD-fed male and female $A_{2A}R$-disrupted mice and their WT littermates. During and after MCD feeding period, all mice revealed significant decreases in body weight regardless of $A_{2A}R$ disruption and sex of the mice. Also, all mice started to consume fewer foods after MCD feeding

for 2 weeks. However, these changes in $A_{2A}R$-disrupted mice were comparable with those in WT littermates (Fig. 4A and B, data from male mice only). In addition, abdominal fat mass and adiposity in $A_{2A}R$-disrupted mice did not differ significantly from those in WT littermates (Fig. 4C and D). Specifically, epididymal fat mass was 0.079 ± 0.009 g for MCD-$A_{2A}R^{-/-}$ mice, 0.078 ± 0.0064 g for MCD-$A_{2A}R^{+/-}$ mice, and 0.061 ± 0.006 g for MCD-$A_{2A}R^{+/+}$ mice (data from male mice only). These results suggest that $A_{2A}R$ disruption did not significantly alter MCD-induced decreases in body weight and abdominal fat mass.

$A_{2A}R$ disruption exacerbates MCD-induced hepatic steatosis and inflammation

MCD feeding induces NASH while decreasing liver weight. In the present study, the levels of plasma ALT in MCD-fed male $A_{2A}R^{-/-}$ mice were significantly higher than those in MCD-fed male $A_{2A}R^{+/+}$ mice (Fig. 5A). Also, liver weight of $A_{2A}R$-disrupted male mice was greater than that in WT male mice (Fig. 5B), although all mice revealed significant decreases in liver weight relative to CD-fed mice. Compared with male $A_{2A}R^{+/+}$ mice, male $A_{2A}R$-disrupted mice also revealed a significant increase in the severity of MCD-induced hepatic steatosis, indicated by the results from liver sections stained with H&E and/or Oil Red O (Fig. 5C). Furthermore, the severity of MCD-induced hepatic steatosis in male $A_{2A}R^{-/-}$ mice was greater than in male $A_{2A}R^{+/-}$ mice. Male $A_{2A}R$-disrupted mice also displayed a significant increase in accumulation of liver macrophages/Kupffer cells. This increase in male $A_{2A}R^{-/-}$ mice was much greater than in male $A_{2A}R^{+/-}$ mice. Of note, macrophages/Kupffer cells were aggregated in large groups in livers of MCD-fed male $A_{2A}R^{-/-}$ mice. When inflammatory signaling was analyzed, the phosphorylation states of JNK p46 and NFκB p65 were increased in MCD-fed male $A_{2A}R^{-/-}$ or $A_{2A}R^{+/-}$ mice compared with MCD-fed male $A_{2A}R^{+/+}$ mice (Fig. 5D). Additionally, MCD-fed male $A_{2A}R^{-/-}$ or $A_{2A}R^{+/-}$ mice displayed significant increases in *Tnfa*, *Il1b*, and *Il6* mRNAs (Fig. 5E). Next, we analyzed the expression of lipogenic genes/enzymes and observed that hepatic *Acc1*, *Fas*, and *Srebp1c* mRNAs in MCD-fed male $A_{2A}R^{-/-}$ mice were significantly higher than their respective levels in MCD-fed male $A_{2A}R^{+/+}$ mice, whereas *Cpt1a* mRNAs in MCD-fed male $A_{2A}R^{-/-}$ or $A_{2A}R^{+/-}$ mice did not differ from those in MCD-fed male $A_{2A}R^{+/+}$ mice (Fig. 5E). These results suggest that $A_{2A}R$ disruption exacerbates NASH phenotype in MCD-fed male mice. In female mice, we observed similar phenotype upon MCD feeding (data not shown).

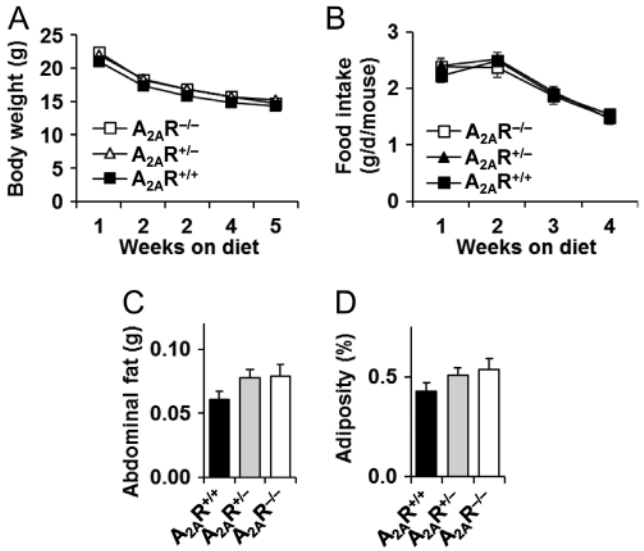

Figure 4
A2AR disruption does not alter MCD-induced decreases in body weight and adiposity. Male $A_{2A}R^{-/-}$ mice, $A_{2A}R^{+/-}$ mice, and $A_{2A}R^{+/+}$ mice, at 9–10 weeks of age, were fed an MCD for 5 weeks or maintained on a CD. (A and B) During the feeding period, body weight of the mice was measured (A). Also, foods consumed by the mice were recorded during the feeding period and used to calculate food intake (B). (C) After harvest, the mass of epididymal, mesenteric, and perinephric fats was estimated as abdominal fats. (D) Adiposity was calculated by normalizing abdominal fats with body weight. For A, B, C and D, data are means ± S.E.M. n = 8–10.

$A_{2A}R$-disrupted macrophages, but not hepatocytes, reveal increased proinflammatory responses upon incubation with MCD-mimicking media

$A_{2A}R$ deficiency exacerbated MCD-induced liver inflammation. Considering that $A_{2A}R$-deficient mice lacked $A_{2A}R$ in both hepatocytes and macrophages, we sought to determine the direct effects of MCD-mimicking media on the proinflammatory responses of $A_{2A}R$-deficient hepatocytes and/or macrophages. Upon incubation with MCD-mimicking media, primary hepatocytes from either $A_{2A}R^{-/-}$ mice or $A_{2A}R^{+/+}$mice did not reveal significant changes in LPS-induced phosphorylation states of JNK1 p46 and NFκB p65 compared with hepatocytes incubated with control media (Fig. 6A), suggesting that MCD-mimicking media have limited effects on altering hepatocyte proinflammatory responses regardless of the presence or absence of $A_{2A}R$. In contrast, incubation with MCD-mimicking media caused a significant increase in LPS-induced phosphorylation states of NFκB p65 in $A_{2A}R^{+/+}$-BMDM (Fig. 6B) relative to control media. Moreover, upon incubation with MCD-mimicking media, $A_{2A}R^{-/-}$-BMDM revealed significant increases in

https://joe.bioscientifica.com
https://doi.org/10.1530/JOE-19-0198

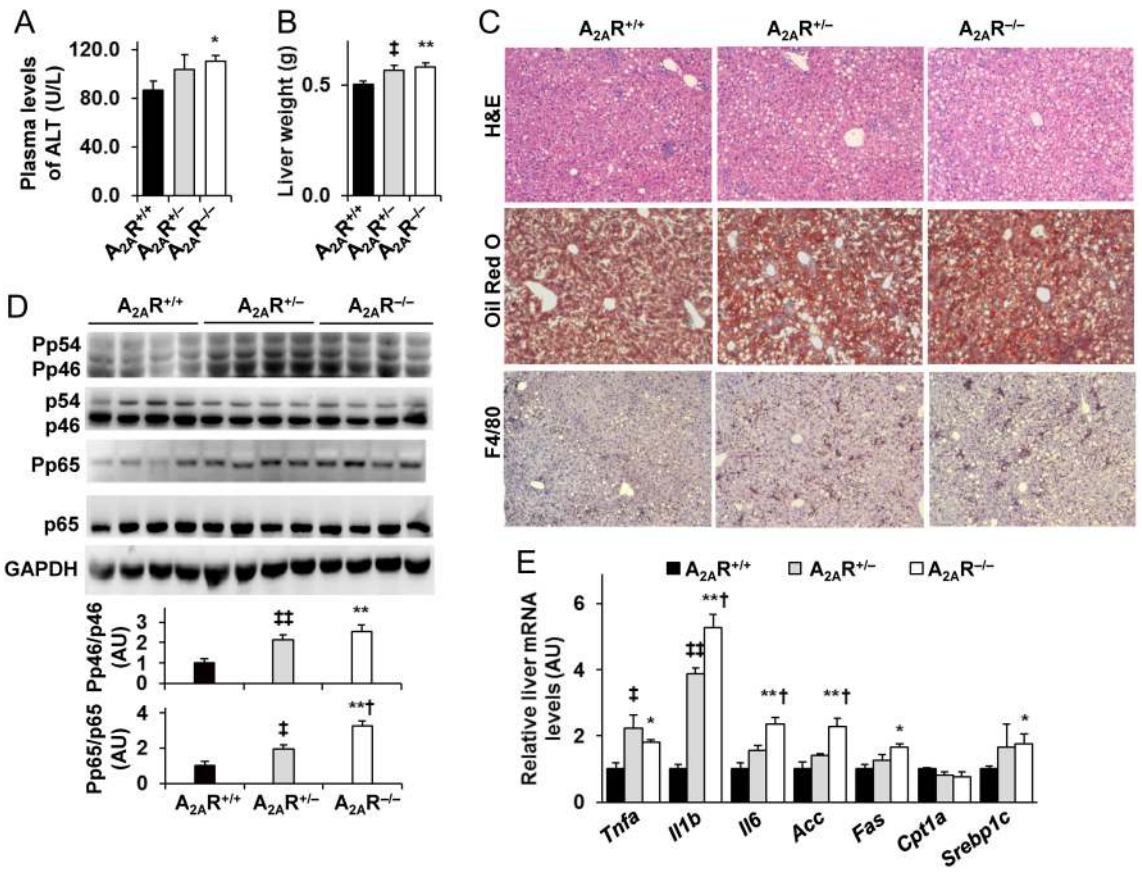

Figure 5
A2AR disruption exacerbates MCD-induced hepatic steatosis and inflammation. Male $A_{2A}R^{-/-}$ mice, $A_{2A}R^{+/-}$ mice, and $A_{2A}R^{+/+}$ mice, at 9–10 weeks of age, were fed an MCD for 5 weeks or maintained on a CD. (A) Plasma levels of ALT. (B) Liver weight. (C) Liver sections were stained with H&E or Oil Red O or for F4/80. (D) Liver lysates were examined for the phosphorylation states of JNK p46 and NFκB p65. Bar graphs, quantification of blots. (E) Liver mRNA levels were examined using real-time PCR. For A, B, D, and E, numeric data are means ± S.E.M. n = 8–10 (A and B) or 6–8 (D and E). AU, arbitrary unit. $^{*}P < 0.05$ and $^{**}P < 0.01$ A2AR$^{-/-}$ vs. $A_{2A}R^{+/+}$ (in A and B, and in bar graphs of D) for the same gene (in E); $^{\dagger}P < 0.05$ A2AR$^{-/-}$ vs $A_{2A}R^{+/-}$ (in D, bar graphs) for the same gene (in E); $^{\ddagger}P < 0.05$ and $^{\ddagger\ddagger}P < 0.01$ A2AR$^{+/-}$ vs $A_{2A}R^{+/+}$ (in B and bar graphs of D) for the same gene (in D). A full colour version of this figure is available at https://doi.org/10.1530/JOE-19-0198.

LPS-induced phosphorylation states of p38 and NFκB p65 compared with $A_{2A}R^{+/+}$-BMDM (Fig. 6B). Since MCD increased NFκB p65 phosphorylation in WT BMDM but not $A_{2A}R^{-/-}$ BMDM, we next measured cytokine expression in WT BMDM incubated with MCD-mimicking media or control media. Compared with control, MCD-mimicking media significantly increased *Tnfa*, *Il1b*, and *Il6* mRNAs (Fig. 6C). In a confirmatory study involving RAW264.7 cells, incubation with MCD-mimicking media caused significant increases in the phosphorylation states of JNK p46 and/or NFκB p65 relative to control media under both basal and LPS-stimulated conditions (Fig. 6D). Additionally, *Tnfa*, *Il1b*, and *Il6* mRNAs in MCD-mimicking media-treated RAW264.7 cells were significantly higher than their respective levels in control media-treated RAW264.7 cells (Fig. 6E). These results suggest that MCD-mimicking media enhance the proinflammatory responses in macrophages, but not hepatocytes.

Discussion

The prevalence of NAFLD is markedly increased among obese subjects due to, in large part, adiposity-associated overflow of fats and adipokines/cytokines to the liver to trigger or exacerbate hepatic steatosis and inflammation (Nugent & Younossi 2007, van der Poorten *et al.* 2008, Estes *et al.* 2018). Interestingly, there also is a good amount of evidence suggesting the presence of NAFLD/NASH in lean subjects (Feldman *et al.* 2017, Kim *et al.* 2019), in which genetic factors, but not obesity-related factors, are thought to contribute to the pathogenesis of

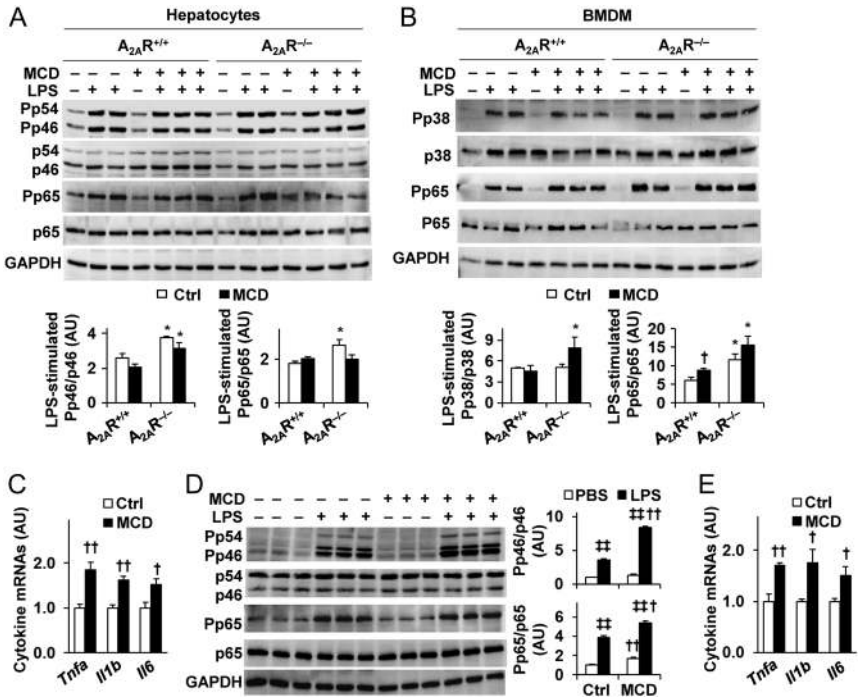

Figure 6
$A_{2A}R$ deficiency enhances the effect of MCD-mimicking media on stimulating proinflammatory responses in macrophages, but not hepatocytes. (A, B and C) Proinflammatory signaling (A and B) and cytokine expression (C) in primary hepatocytes (A) and bone marrow-derived macrophages (BMDM) (B and C). For A, B and C, male $A_{2A}R^{-/-}$ mice and $A_{2A}R^{+/+}$ mice, at 10–12 weeks of age, were subjected to isolation of primary hepatocytes and bone marrow cells. Primary hepatocytes and BMDM were treated with MCD-mimicking media for 24 h in the presence or absence of LPS (100 ng/mL) for the last 30 min (A and B) or LPS (20 ng/mL) for the last 6 h. (D and E) Proinflammatory signaling (D) and cytokine expression (E) in RAW264.7 cells. At 80% confluence, RAW264.7 cells were incubated with MCD-mimicking media or control media for 24 h in the presence or absence of LPS (100 ng/mL) for the last 30 min (D) or LPS (20 ng/mL) for the last 6 h. For A, B, and D, cell lysates were examined for proinflammatory signaling using Western blot analysis. Bar graphs, quantification of blots. For all bar graphs, data are means ± s.e., $n = 4$–6. AU, arbitrary unit. $^{*}P < 0.05$ A2AR$^{-/-}$ vs $A_{2A}R^{+/+}$ under the same condition (Ctrl or MCD, in A and B); $^{\dagger}P < 0.05$ and $^{\dagger\dagger}P < 0.01$ MCD vs Ctrl within the same genotype (in B) or for the same gene (in C and E) or under the same condition (PBS or LPS, in D); $^{\ddagger}P < 0.05$ and $^{\ddagger\ddagger}P < 0.01$ LPS vs PBS within the same media (in D).

NAFLD/NASH. Similarly, the prevalence of NAFLD/NASH or even liver fibrosis is also increased among HIV-infected patients who have normal BMI or lipodystrophy (Pérez-Matute *et al.* 2013, van Welzen *et al.* 2019). In this case, HIV infection-related inflammation is considered as a key factor to drive the pathogenesis of NAFLD/NASH or liver fibrosis, although the precise underlying mechanisms remain to be elucidated. To date, there is a lack of a perfect animal model for studying NAFLD pathophysiology in the absence of obesity or in the presence of lipodystrophy. Because feeding an MCD to C57BL/6 mice causes severe hepatic steatosis and inflammation while causing lipoatrophy, we analyzed changes in hepatic expression of $A_{2A}R$ in MCD-fed mice and examined the effect of $A_{2A}R$ disruption on MCD-induced NASH phenotype.

Similar to HFD-fed C57BL/6J mice (Cai *et al.* 2018), MCD-fed C57BL/6J mice displayed hepatic steatosis relative to chow diet-fed mice. However, the severity of liver inflammation in MCD-fed C57BL/6J mice was much greater than that in HFD-fed C57BL/6J mice, which is consistent with our previous report (Luo *et al.* 2018). In particular, liver sections of MCD-fed C57BL/6J mice contained significantly more F4/80-positive cells, many of which were aggregated. In addition, MCD-fed C57BL/6J mice contained almost no fat mass, in particular visceral fat mass. These characteristics not only validated MCD-fed C57BL/6J mice as a model for studying NASH in the presence of lipoatrophy, but also indicated that MCD-fed mice developed liver inflammation via mechanism(s) different from those for HFD-fed mice. As supporting evidence, hepatic expression of $A_{2A}R$, an ant-inflammatory molecule, was differentially regulated in MCD-fed mice compared with HFD-fed mice. Specifically, $A_{2A}R$ abundance in liver lysates, unlike that in liver lysates of HFD-C57BL/6J fed mice (Cai *et al.* 2018), was decreased in MCD-fed C57BL/6J mice. Upon examining $A_{2A}R$ expression using immunofluorescence staining, we showed that liver sections of MCD-fed mice, indeed, contained significant more $A_{2A}R$-postive cells than those of CD-fed mice. Because most $A_{2A}R$-postive cells were F4/80-positive cells, we argued that MCD feeding increased $A_{2A}R$ expression in macrophages, although it decreased whole liver $A_{2A}R$ abundance. The latter may be attributable to decreased $A_{2A}R$ expression in hepatocytes, which is opposite to that in HFD-fed mice where $A_{2A}R$ expression was increased in hepatocytes (Cai *et al.* 2018). Considering that $A_{2A}R$ exerts powerful anti-inflammatory effects, we speculated that the $A_{2A}R$ in macrophages could play a more important role than the $A_{2A}R$ in hepatocyte in terms of regulating liver inflammation in MCD-fed mice.

https://joe.bioscientifica.com
https://doi.org/10.1530/JOE-19-0198

This concept was substantiated by the differences in the responses of hepatocytes versus macrophages to culture media mimicking MCD (see below).

Activation of $A_{2A}R$ by an agonist has been shown to ameliorate MCD-induced NASH phenotype in both rats and mice (Imarisio *et al.* 2012, Alchera *et al.* 2017). Considering this, we speculated that the decrease in $A_{2A}R$ amount in liver lysates of MCD-fed mice was indicative of reduced protection of NASH phenotype, although $A_{2A}R$ expression was increased in macrophages/Kupffer cells of liver sections from MCD-fed mice. In agreement with our speculation, $A_{2A}R$-deficient mice revealed significant increases in the severity of MCD-induced hepatic steatosis and inflammation compared with WT control mice. Of note, the severity of hepatic steatosis in MCD-fed homozygous $A_{2A}R$-deficient mice, indicated by the results of liver histology, was significantly greater than that in MCD-fed heterozygous $A_{2A}R$-disrupted mice. Moreover, the degrees of liver inflammation in MCD-fed homozygous $A_{2A}R$-deficient mice, indicated by the numbers of F4/80-postivie macrophages/Kupffer cells, the phosphorylation states of NF-κB p65, and the mRNA levels of *Il1b* and *Il6*, in livers from MCD-fed homozygous $A_{2A}R$-deficient mice were also significantly higher than their respective levels in MCD-fed heterozygous $A_{2A}R$-disrupted mice. These findings, along with the results indicative of increased severity of NASH phenotype in heterozygous $A_{2A}R$-dirupted mice relative to that in WT mice, strongly suggest that $A_{2A}R$ exerts a gene-dose-dependent effect on protecting against MCD-induced NASH phenotype. What should be noted is that $A_{2A}R$ exerts a similarly gene-dose-dependent effect on protecting against NAFLD phenotype in obese mice (Cai *et al.* 2018), where inflammation, but not adiposity, is the characteristic shared by MCD-fed mice. Therefore, the anti-inflammatory effect of $A_{2A}R$ likely accounts for, to a large extent, protection of NASH in MCD-fed mice.

In MCD-fed mice, $A_{2A}R$ expression was increased in liver macrophages/Kupffer cells. This increase appeared to a defensive response and was different from the $A_{2A}R$ in non-macrophages/Kupffer cells where decreased $A_{2A}R$ expression might be a consequence or adaptive response to MCD feeding. In other words, it is possible that upon MCD feeding macrophage $A_{2A}R$ expression was increased to counter against massive inflammation whereas the $A_{2A}R$ in other cells, mainly, hepatocytes, was decreased and contributed to increases in hepatocyte fat deposition and proinflammatory responses. At this point, the mechanisms by which MCD feeding differentially regulates $A_{2A}R$ expression in macrophages/Kupffer cells and other cells, for example, hepatocytes, are not clear. However, MCD feeding appears to primarily account for decreasing hepatocyte $A_{2A}R$ expression; considering that HFD feeding increases hepatocyte $A_{2A}R$ expression (Cai *et al.* 2018). To be noted, methionine and choline are key nutrients involved in methionine cycle and methylation reactions. Given this, alterations of hepatocyte methylation reactions in response to deficiency of methionine and choline in diet likely are MCD-induced upstream events of hepatocyte $A_{2A}R$ expression. This view, however, is in need of validation by future study. Nonetheless, the differential expression of $A_{2A}R$ in different liver cells led us to examine the effect of MCD-mimicking media on the direct responses of macrophages versus hepatocytes. Indeed, we validated that MCD-mimicking media generated different effects on proinflammatory responses in the two types of cells. Notably, MCD-mimicking media increased LPS-induced phosphorylation states of NFκB p65 in WT macrophages and insignificant increases in the phosphorylation states of p38 and NFκB p65 in $A_{2A}R$-deficeint macrophages. In contrast, MCD-mimicking media did not significantly alter or even tended to decrease LPS-induced phosphorylation states of JNK p46 and/or NFκB p65 in both WT and $A_{2A}R$-deficient hepatocytes. Because of this, we speculated that the $A_{2A}R$ in macrophages directly responded to MCD feeding in a defensive manner to exert an anti-inflammatory effect. However, future study is needed to examine the extent to which $A_{2A}R$ disruption only in myeloid cells also protects against MCD-induced NASH phenotype.

In summary, we validated that $A_{2A}R$ expression was increased in liver macrophages/Kupffer cells, but was decreased in liver lysates of MCD-fed WT mice. We then demonstrated a protective role for $A_{2A}R$ in MCD-induced NASH phenotype. At the cellular level, the $A_{2A}R$ in macrophages appears to be more important than that in hepatocytes in terms of suppressing the effect of MCD or MCD-mimicking media on stimulating the proinflammatory responses. Therefore, we provide additional evidence supporting the potential of targeting $A_{2A}R$ to suppress liver inflammation as a therapeutic strategy for the treatment of NASH.

Declaration of interest

The authors declare that there is no conflict of interest that could be perceived as prejudicing the impartiality of the research reported.

https://joe.bioscientifica.com
https://doi.org/10.1530/JOE-19-0198

Funding

This work was supported in whole or in part by grants from the American Diabetes Association (1-17-IBS-145 to C W) and the National Institutes of Health (DK095862 to C W). Also, C W is supported by the Hatch Program of the National Institutes of Food and Agriculture (NIFA). Y Chen is supported by grants from China National Science Foundation (81770826) and Guangzhou Science and Technology Plan (2060404). X Q is supported by Guangdong Province Science and Technology Plan (2016A050502014).

Author contribution statement

J Z carried out most of animal experiments. H L carried out all histological and immunochemical assays. Y Cai, L M, D M, B L, B Z, and L Z collected tissue and cell samples, performed molecular and biochemical assays, and analyzed the data. C W came up the concept of the study. Y Chen, X Q, X X, Qifu L, S G, Y H, L Z, Y T, and Qingsheng L contributed to scientific discussion. C W supervised all experiments and wrote the manuscript.

References

Alchera E, Rolla S, Imarisio C, Bardina V, Valente G, Novelli F & Carini R 2017 Adenosine A2a receptor stimulation blocks development of nonalcoholic steatohepatitis in mice by multilevel inhibition of signals that cause immunolipotoxicity. *Translational Research* **182** 75–87. (https://doi.org/10.1016/j.trsl.2016.11.009)

Browning JD, Szczepaniak LS, Dobbins R, Nuremberg P, Horton JD, Cohen JC, Grundy SM & Hobbs HH 2004 Prevalence of hepatic steatosis in an urban population in the United States: impact of ethnicity. *Hepatology* **40** 1387–1395. (https://doi.org/10.1002/hep.20466)

Bugianesi E, Leone N, Vanni E, Marchesini G, Brunello F, Carucci P, Musso A, De Paolis P, Capussotti L, Salizzoni M, *et al.* 2002 Expanding the natural history of nonalcoholic steatohepatitis: from cryptogenic cirrhosis to hepatocellular carcinoma. *Gastroenterology* **123** 134–140. (https://doi.org/10.1053/gast.2002.34168)

Cai Y, Li H, Liu M, Pei Y, Zheng J, Zhou J, Luo X, Huang W, Ma L, Yang Q, *et al.* 2018 Disruption of adenosine 2A receptor exacerbates NAFLD through increasing inflammatory responses and SREBP1c activity. *Hepatology* **68** 48–61. (https://doi.org/10.1002/hep.29777)

Chalasani N, Younossi Z, Lavine JE, Charlton M, Cusi K, Rinella M, Harrison SA, Brunt EM & Sanyal AJ 2018 The diagnosis and management of nonalcoholic fatty liver disease: practice guidance from the American Association for the Study of Liver Diseases. *Hepatology* **67** 328–357. (https://doi.org/10.1002/hep.29367)

Cohen JC, Horton JD & Hobbs HH 2011 Human fatty liver disease: old questions and new insights. *Science* **332** 1519–1523. (https://doi.org/10.1126/science.1204265)

Csóka B, Törő G, Vindeirinho J, Varga ZV, Koscsó B, Németh ZH, Kókai E, Antonioli L, Suleiman M, Marchetti P, *et al.* 2017 A2A adenosine receptors control pancreatic dysfunction in high-fat-diet-induced obesity. *FASEB Journal* **31** 4985–4997. (https://doi.org/10.1096/fj.201700398R)

Estes C, Razavi H, Loomba R, Younossi Z & Sanyal AJ 2018 Modeling the epidemic of nonalcoholic fatty liver disease demonstrates an exponential increase in burden of disease. *Hepatology* **67** 123–133. (https://doi.org/10.1002/hep.29466)

Feldman A, Eder SK, Felder TK, Kedenko L, Paulweber B, Stadlmayr A, Huber-Schönauer U, Niederseer D, Stickel F, Auer S, *et al.* 2017 Clinical and metabolic characterization of lean Caucasian subjects with non-alcoholic fatty liver. *American Journal of Gastroenterology* **112** 102–110. (https://doi.org/10.1038/ajg.2016.318)

Gessi S, Varani K, Merighi S, Ongini E & Borea PA 2000 A2A adenosine receptors in human peripheral blood cells. *British Journal of Pharmacology* **129** 2–11. (https://doi.org/10.1038/sj.bjp.0703045)

Guo X, Xu K, Zhang J, Li H, Zhang W, Wang H, Lange AJ, Chen YE, Huo Y & Wu C 2010 Involvement of inducible 6-phosphofructo-2-kinase in the anti-diabetic effect of peroxisome proliferator-activated receptor γ activation in mice. *Journal of Biological Chemistry* **285** 23711–23720. (https://doi.org/10.1074/jbc.M110.123174)

Guo X, Li H, Xu H, Halim V, Zhang W, Wang H, Ong KT, Woo SL, Walzem RL, Mashek DG, *et al.* 2012 Palmitoleate induces hepatic steatosis but suppresses liver inflammatory response in mice. *PLoS ONE* **7** e39286. (https://doi.org/10.1371/journal.pone.0039286)

Guo X, Li H, Xu H, Halim V, Thomas LN, Woo SL, Huo Y, Chen YE, Sturino JM & Wu C 2013 Disruption of inducible 6-phosphofructo-2-kinase impairs the suppressive effect of PPARγ activation on diet-induced intestine inflammatory response. *Journal of Nutritional Biochemistry* **24** 770–775. (https://doi.org/10.1016/j.jnutbio.2012.04.007)

Guo T, Woo SL, Guo X, Li H, Zheng J, Botchlett R, Liu M, Pei Y, Xu H, Cai Y, *et al.* 2016 Berberine ameliorates hepatic steatosis and suppresses liver and adipose tissue inflammation in mice with diet-induced obesity. *Scientific Reports* **6** 22612. (https://doi.org/10.1038/srep22612)

Haskó G, Linden J, Cronstein B & Pacher P 2008 Adenosine receptors: therapeutic aspects for inflammatory and immune diseases. *Nature Reviews. Drug Discovery* **7** 759–770. (https://doi.org/10.1038/nrd2638)

Huo Y, Guo X, Li H, Wang H, Zhang W, Wang Y, Zhou H, Gao Z, Telang S, Chesney J, *et al.* 2010 Disruption of inducible 6-phosphofructo-2-kinase ameliorates diet-induced adiposity but exacerbates systemic insulin resistance and adipose tissue inflammatory response. *Journal of Biological Chemistry* **285** 3713–3721. (https://doi.org/10.1074/jbc.M109.058446)

Huo Y, Guo X, Li H, Xu H, Halim V, Zhang W, Wang H, Fan YY, Ong KT, Woo SL, *et al.* 2012 Targeted overexpression of inducible 6-phosphofructo-2-kinase in adipose tissue increases fat deposition but protects against diet-induced insulin resistance and inflammatory responses. *Journal of Biological Chemistry* **287** 21492–21500. (https://doi.org/10.1074/jbc.M112.370379)

Imarisio C, Alchera E, Sutti S, Valente G, Boccafoschi F, Albano E & Carini R 2012 Adenosine A2a receptor stimulation prevents hepatocyte lipotoxicity and nonalcoholic steatohepatitis (NASH) in rats. *Clinical Science* **123** 323–332. (https://doi.org/10.1042/CS20110504)

Kamei N, Tobe K, Suzuki R, Ohsugi M, Watanabe T, Kubota N, Ohtsuka-Kowatari N, Kumagai K, Sakamoto K, Kobayashi M, *et al.* 2006 Overexpression of monocyte chemoattractant protein-1 in adipose tissues causes macrophage recruitment and insulin resistance. *Journal of Biological Chemistry* **281** 26602–26614. (https://doi.org/10.1074/jbc.M601284200)

Kang K, Reilly SM, Karabacak V, Gangl MR, Fitzgerald K, Hatano B & Lee CH 2008 Adipocyte-derived Th2 cytokines and myeloid PPARδ regulate macrophage polarization and insulin sensitivity. *Cell Metabolism* **7** 485–495. (https://doi.org/10.1016/j.cmet.2008.04.002)

Kelley DE, McKolanis TM, Hegazi RAF, Kuller LH & Kalhan SC 2003 Fatty liver in type 2 diabetes mellitus: relation to regional adiposity, fatty acids, and insulin resistance. *American Journal of Physiology-Endocrinology and Metabolism* **285** E906–E916. (https://doi.org/10.1152/ajpendo.00117.2003)

Kim D, Kim W, Joo SK, Kim JH, Harrison SA, Younossi ZM & Ahmed A 2019 Predictors of nonalcoholic steatohepatitis and significant fibrosis in non-obese nonalcoholic fatty liver disease. *Liver International* **39** 332–341. (https://doi.org/10.1111/liv.13983)

Luo X, Li H, Ma L, Zhou J, Guo X, Woo SL, Pei Y, Knight LR, Deveau M, Chen Y, *et al.* 2018 Expression of STING is increased in liver tissues from patients with NAFLD and promotes macrophage-mediated

hepatic inflammation and fibrosis in mice. *Gastroenterology* **155** 1971–1984.e4. (https://doi.org/10.1053/j.gastro.2018.09.010)

Marrero JA, Fontana RJ, Su GL, Conjeevaram SH, Emick DM & Lok AS 2002 NAFLD may be a common underlying liver disease in patients with hepatocellular carcinoma in the United States. *Hepatology* **36** 1349–1354.

Menghini R, Menini S, Amoruso R, Fiorentino L, Casagrande V, Marzano V, Tornei F, Bertucci P, Iacobini C, Serino M, *et al*. 2009 Tissue inhibitor of metalloproteinase 3 deficiency causes hepatic steatosis and adipose tissue inflammation in mice. *Gastroenterology* **136** 663.e4–672.e4. (https://doi.org/10.1053/j.gastro.2008.10.079)

Neuschwander-Tetri BA 2010 NASH: thiazolidinediones for NASH--one pill doesn't fix everything. *Nature Reviews Gastroenterology and Hepatology* **7** 243–244. (https://doi.org/10.1038/nrgastro.2010.50)

Nugent C & Younossi ZM 2007 Evaluation and management of obesity-related nonalcoholic fatty liver disease. *Nature Clinical Practice Gastroenterology and Hepatology* **4** 432–441. (https://doi.org/10.1038/ncpgasthep0879)

Odegaard JI, Ricardo-Gonzalez RR, Red Eagle A, Vats D, Morel CR, Goforth MH, Subramanian V, Mukundan L, Ferrante AW & Chawla A 2008 Alternative M2 activation of Kupffer cells by PPARδ ameliorates obesity-induced insulin resistance. *Cell Metabolism* **7** 496–507. (https://doi.org/10.1016/j.cmet.2008.04.003)

Pei Y, Li H, Cai Y, Zhou J, Luo X, Ma L, McDaniel K, Zeng T, Chen Y, Qian X, *et al*. 2018 Regulation of adipose tissue inflammation by adenosine 2A receptor in obese mice. *Journal of Endocrinology* **239** 365–376.

Pérez-Matute P, Pérez-Martínez L, Blanco JR & Oteo JA 2013 Role of mitochondria in HIV infection and associated metabolic disorders: focus on nonalcoholic fatty liver disease and lipodystrophy syndrome. *Oxidative Medicine and Cellular Longevity* **2013** 493413. (https://doi.org/10.1155/2013/493413)

Powell EE, Jonsson JR & Clouston AD 2005 Steatosis: co-factor in other liver diseases. *Hepatology* **42** 5–13. (https://doi.org/10.1002/hep.20750)

Qi T, Chen Y, Li H, Pei Y, Woo SL, Guo X, Zhao J, Qian X, Awika J, Huo Y, *et al*. 2017 2017 A role for PFKFB3/iPFK2 in metformin suppression of adipocyte inflammatory responses. *Journal of Molecular Endocrinology* **59** 49–59. (https://doi.org/10.1530/JME-17-0066)

Rinella ME, Elias MS, Smolak RR, Fu T, Borensztajn J & Green RM 2008 Mechanisms of hepatic steatosis in mice fed a lipogenic methionine choline-deficient diet. *Journal of Lipid Research* **49** 1068–1076. (https://doi.org/10.1194/jlr.M800042-JLR200)

Sanyal AJ 2005 Mechanisms of disease: pathogenesis of nonalcoholic fatty liver disease. *Nature Clinical Practice Gastroenterology and Hepatology* **2** 46–53. (https://doi.org/10.1038/ncpgasthep0084)

Schaffler A, Scholmerich J & Buchler C 2005 Mechanisms of disease: adipocytokines and visceral adipose tissue – emerging role in nonalcoholic fatty liver disease. *Nature Clinical Practice Gastroenterology and Hepatology* **2** 273–280. (https://doi.org/10.1038/ncpgasthep0186)

Starley BQ, Calcagno CJ & Harrison SA 2010 Nonalcoholic fatty liver disease and hepatocellular carcinoma: a weighty connection. *Hepatology* **51** 1820–1832. (https://doi.org/10.1002/hep.23594)

Tilg H & Moschen AR 2010 Evolution of inflammation in nonalcoholic fatty liver disease: the multiple parallel hits hypothesis. *Hepatology* **52** 1836–1846. (https://doi.org/10.1002/hep.24001)

van der Poorten D, Milner KL, Hui J, Hodge A, Trenell MI, Kench JG, London R, Peduto T, Chisholm DJ & George J 2008 Visceral fat: a key mediator of steatohepatitis in metabolic liver disease. *Hepatology* **48** 449–457. (https://doi.org/10.1002/hep.22350)

van Welzen BJ, Mudrikova T, El Idrissi A, Hoepelman AIM & Arends JE 2019 A review of non-alcoholic fatty liver disease in HIV-infected patients: the next big thing? *Infectious Diseases and Therapy* **8** 33–50. (https://doi.org/10.1007/s40121-018-0229-7)

Xu H, Li H, Woo SL, Kim SM, Shende VR, Neuendorff N, Guo X, Guo T, Qi T, Pei Y, *et al*. 2014 Myeloid cell-specific disruption of Period1 and Period2 exacerbates diet-induced inflammation and insulin resistance. *Journal of Biological Chemistry* **289** 16374–16388. (https://doi.org/10.1074/jbc.M113.539601)

Younossi ZM, Koenig AB, Abdelatif D, Fazel Y, Henry L & Wymer M 2016 Global epidemiology of nonalcoholic fatty liver disease-Meta-analytic assessment of prevalence, incidence, and outcomes. *Hepatology* **64** 73–84. (https://doi.org/10.1002/hep.28431)

Received in final form 1 August 2019
Accepted 6 September 2019
Accepted Preprint published online 6 September 2019